Journal of Applied Mechanics and Technical Physics, Vol. 49, No. 3, pp. 400–406, 2008

EFFECT OF THE ACCOMMODATION COEFFICIENT ON TRANSFER PROCESSES IN A SUPERSONIC RAREFIED GAS FLOW AROUND A TRANSVERSELY ALIGNED CYLINDER

M. Yu. Plotnikov

UDC 533.7:532.546

A supersonic flow around a cylinder is studied by the direct statistical Monte Carlo method in a wide range of rarefaction: from regimes close to continuum to free-molecular flow. The effect of the accommodation coefficient on the flow near the cylinder and on heat transfer between the gas and the cylinder is examined.

Key words: *supersonic flow, flow around a cylinder, heat transfer, direct statistical Monte Carlo* (DSMC) *method, accommodation coefficient.*

The study of a supersonic rarefied gas flow around a cylinder has attracted attention of researchers since the 1950s [1, 2]. The possibilities of the numerical solution of this problem have been recently enhanced by the development of numerical methods of gas dynamics on one hand and by the evolution of computational engineering on the other hand. The flow around a cylinder was numerically studied by solving the Navier–Stokes equations in [3, 4]. The variable soft sphere (VSS) model was tested in [5] in the case of direct statistical Monte Carlo (DSMC) simulations [6] of a nitrogen flow around a cylinder. The influence of internal degrees of freedom of molecules on the flow field and on heat transfer in a hypersonic rarefied gas flow around a cylinder was considered in [7]. The specific features of a flow of a binary mixture of gases around a cylinder was studied in [8] by the DSMC method.

The present paper is a continuation of [9] where the technique of determining the accommodation coefficient in a supersonic free-molecular flow around a thin-wire probe [10, 11] was numerically justified. The technique is based on studying heat fluxes in a free-molecular flow around the wire; hence, a question arises on choosing flow regimes with heat transfer between the gas and the cylinder close to heat transfer in the free-molecular regime. The effect of the degree of flow rarefaction on the flow structure and on heat transfer was evaluated in [9].

The main objective of the present work was the study of a supersonic rarefied gas flow around a transversely aligned cylinder of infinite length, aimed at estimating the influence of the accommodation coefficient on the flow structure and on heat transfer. An additional recent impetus for such a research was the development of the gas-dynamic method of thin-film deposition in vacuum [12–14] and the associated necessity of a detailed study of essentially nonequilibrium regions near the coated surfaces of different configurations.

1. Formulation of the Problem and Solution by the DSMC Method. We used a rectangular coordinate system (X, Y, Z), where the X axis was directed downstream and the Y and Z axes were perpendicular to the flow (the Z axis coincided with the cylinder centerline).

We considered a steady plane-parallel supersonic flow of a monatomic gas around an infinite cylinder of diameter d. The plane source was located in the cross section $x = x_s < 0$. The gas was completely absorbed at a certain distance $x = x_e$ further downstream. As the problem is symmetric, we used the following conditions: the plane $y = 0$ was assumed to be specular, and the free-stream boundary conditions were set in the plane $y = y_e$. If a particle returned to the plane of the source, it was assumed to be absorbed.

Kutateladze Institute of Thermophysics, Siberian Division, Russian Academy of Sciences, Novosibirsk 630090; plotnikov@itp.nsc.ru. Translated from Prikladnaya Mekhanika i Tekhnicheskaya Fizika, Vol. 49, No. 3, pp. 64–72, May–June, 2008. Original article submitted May 18, 2007; revision submitted June 25, 2007.

The following boundary conditions for the gas flow were set on the plane where the source was located: translational temperature T_s, velocity V_s, and number density n_s. The temperature of the cylinder surface T_w was assumed to be constant. The particle interaction was described by the VSS model with parameters corresponding to helium [6]. The interaction of particles with the cylinder surface was described by the model of specular-diffuse reflection with an energy accommodation coefficient α. The particles were assumed to be diffusely reflected from the surface with the energy corresponding to the cylinder temperature with a probability α and to be specularly reflected with a probability $1-\alpha$. The degree of rarefaction was characterized by the Knudsen number $\mathrm{Kn} = L/d$ (L is the mean free path determined by the density n_s and temperature T_s). The problem was converted to dimensionless form by using the following scales: temperature T_s, density n_s, mean free path L, and the most probable thermal velocity of particles at the temperature T_s. The governing parameters of the problem were the Mach number M_s, the ratio of temperatures T_w/T_s, the Knudsen number Kn, and the energy accommodation coefficient α.

Obviously, the size of the computational domain (in particular, the positions of the planes $x = x_e$ and $y = y_e$) affects the results. Beginning from certain values of x_e and y_e, the flow near the cylinder becomes almost independent of the computational domain size; these values were found.

The following macroparameters of the flow were computed: density, Mach number, components of velocity and temperatures in the directions along the flow (T_x and V_x) and perpendicular to the flow (T_y, V_y, T_z, and V_z), mean temperature $T = (T_x + T_y + T_z)/3$, heat flux Q between the gas and the cylinder, and drag coefficient of the cylinder C_x.

The number of particles used at each time step was varied between $3 \cdot 10^5$ and $1.5 \cdot 10^6$. The steady-state solution was constructed on the basis of a large number of repetitions. The accuracy of results was monitored by varying the grid step and the time interval of the DSMC algorithm. The solution was assumed to be “precise” if a further decrease in the grid step and time interval did not lead to changes in computed parameters greater than the statistical error. The algorithm parameters were chosen to stay within a 1% stochastic error of computing the flow macroparameters (except for the region immediately behind the cylinder) and the drag coefficient. In the region directly behind the cylinder, the stochastic error reached approximately 10% because of the low density of the flow. The stochastic error of heat-flux computations was smaller than 0.005.

2. Results of Numerical Experiments. The numerical experiments were performed for the following set of parameters: $0.01 \leqslant \mathrm{Kn} \leqslant \infty$, $0 \leqslant \alpha \leqslant 1$, $0.317 \leqslant T_w/T_s \leqslant 26.700$, and $\mathrm{M}_s = 2.9$ and 5.6. Sometimes it is reasonable to present the data obtained via the temperature normalized to the stagnation temperature T_0. For Mach numbers $\mathrm{M}_s = 2.9$ and 5.6, the stagnation temperatures are $3.8T_s$ and $11.45T_s$, respectively. An important characteristic of the problem is the recovery temperature T_r. For the Mach numbers considered, the recovery temperatures in the free-molecular regime are $4.74T_s$ and $14.3T_s$, respectively [2]. For Mach numbers $\mathrm{M}_s = 2.9$ and 5.6, the main fraction of the total heat content (74 and more than 91%, respectively) in the flow is converted to the kinetic energy of directed motion; hence, qualitative conclusions can be also valid for higher Mach numbers.

2.1. *Distribution of Flow Macroparameters.* A typical pattern observed in a supersonic rarefied flow around a cylinder has the following specific features. A disturbed flow region characterized by strong nonequilibrium is formed around the cylinder. The density substantially increases ahead of the cylinder, and a rarefaction zone is observed behind the cylinder. A significant increase in temperature in a certain vicinity of the cylinder is noted. Behind the cylinder, there is a subsonic flow region, which rapidly becomes supersonic. The distributions of flow macroparameters along the axis of symmetry for different values of the Knudsen number were given in [9]. An analysis of the axial distributions of flow parameters allows important conclusions to be drawn. The temperature anisotropy testifies to significant translational nonequilibrium near the cylinder. For $\mathrm{Kn} = 5$, the changes in parameters are similar to their behavior in a free-molecular flow. As Kn decreases, collisions between the incident and reflected molecules lead to a decrease in T_x and an increase in T_y and T_z. For $\mathrm{Kn} = 0.1$, there are two maximums in the distribution of T_x, which can indicate the beginning of formation of a detached shock wave. A boundary layer is formed near the cylinder surface, where the distributions of flow macroparameters substantially depend on the ratio T_w/T_0. An increase in density and a decrease in the total temperature ahead of the cylinder, as well as an increase in the size of the disturbed flow region (expressed in local mean free paths) are noted with decreasing Knudsen number. A reflected shock wave is formed for $\mathrm{Kn} \leqslant 0.1$.

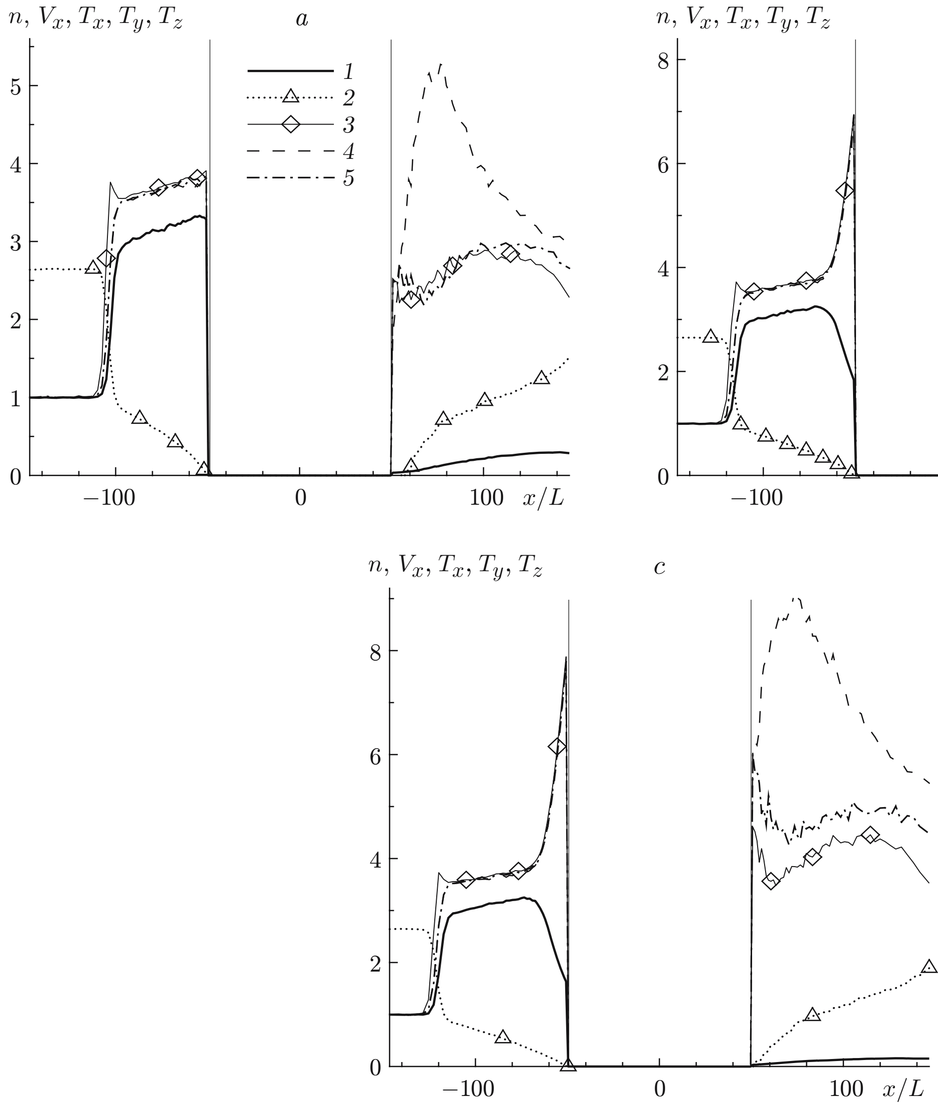

Fig. 1. Distributions of density n (1), velocity V_x (2), and temperatures T_x (3), T_y (4), and T_z (5) over the directions along the plane of symmetry for $\mathrm{M}_s = 2.9$, $\mathrm{Kn} = 0.01$, $T_w/T_0 = 7/3$, and $\alpha = 0$ (a), 0.5 (b), and 1 (c).

Figure 1 shows the distributions of flow macroparameters for $\alpha = 0$ (a), 0.5 (b), and 1.0 (c). The distribution of T_x has a clearly expressed peak ahead of the cylinder and a rather extended, almost equilibrium flow region behind the cylinder. As the accommodation coefficient increases (Figs. 1b and 1c), the fraction of reflected "hot" particles also increases, which alters flow characteristics in the boundary layer. It should be noted that the distribution of parameters in Fig. 1a (specular reflection) is fairly close to the distribution obtained for the same Mach and Knudsen numbers and $T_w/T_0 = 1$ in the case of diffuse reflection of particles. An apparent reason is the absence of energy transfer with the cylinder surface in the first case ($\alpha = 0$) and low-intensity energy transfer in the second case. The changes in macroparameters for $\mathrm{M}_s = 5.6$ are qualitatively similar to those plotted in Fig. 1.

2.2. *Free-Molecular Regime.* For the free-molecular regime, analytical expressions for the drag coefficient C_x^∞, heat flux q^∞, and recovery temperature T_r^∞ [1, 2] are available:

$$C_x^\infty = \frac{\sqrt{\pi}}{3S}\,(4-\alpha)\Big[\Big(S^2+\frac{3}{2}\Big)I_0+\Big(S^2+\frac{1}{2}\Big)I_1\Big]\exp\Big(-\frac{S^2}{2}\Big)+\alpha\,\frac{\pi^{3/2}}{4S}\sqrt{\frac{T_w}{T_s}}\,; \tag{1}$$

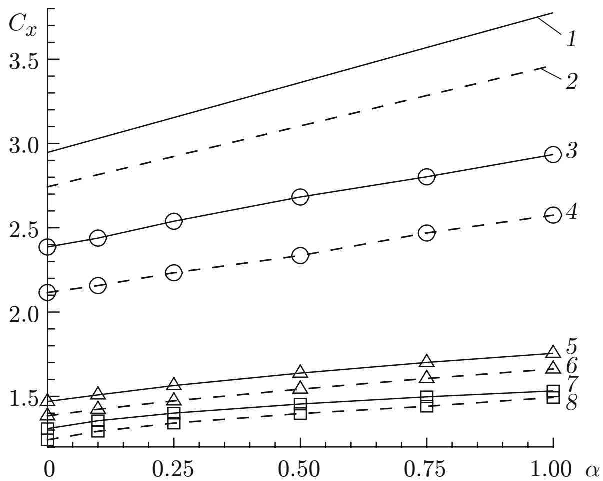

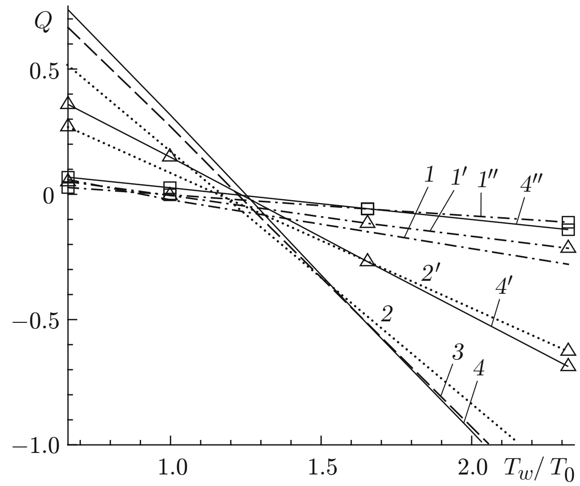

Fig. 2

Fig. 3

Fig. 2. Drag coefficient C_x versus the accommodation coefficient α for different values of the Knudsen number: the solid and dashed curves refer to $\mathrm{M}_s = 2.9$ and 5.6, respectively; $\mathrm{Kn} = \infty$ (1 and 2), 1 (3 and 4), 0.1 (5 and 6), and 0.01 (7 and 8).

Fig. 3. Heat flux versus the ratio of temperatures T_w/T_0 for $\mathrm{M}_s = 2.9$: $\alpha = 1$ (1–4), 0.5 (1′, 2′, and 4′), and 0.1 (1″ and 4″); Kn = 0.01 (1, 1′, and 1″), 1 (2 and 2′), 10 (3), and ∞ (4, 4′, and 4″).

$$q^\infty = (T_r^\infty - T_w)k\alpha n_s\sqrt{2RT_s}\,\frac{1}{\sqrt{\pi}}\,\exp\Big(-\frac{S^2}{2}\Big)[I_0 + S^2(I_0 + I_1)]; \qquad (2)$$

$$T_r^\infty = T_s\Big(\frac{S^2}{2} + \frac{5}{4} - \frac{1}{4 + 4S^2(1 + I_1/I_0)}\Big). \qquad (3)$$

Here $I_0 \equiv I_0(S^2/2)$ and $I_1 \equiv I_1(S^2/2)$ are the zero- and first-order modified Bessel functions of the first kind, $S = \sqrt{5/6}\,\mathrm{M}_s$, and k is the Boltzmann constant; the heat flux q^∞ is normalized to the unit area of the cylinder surface.

The drag coefficient and the heat flux were calculated in the present work by summing the momentum and kinetic energy of particles that collided with the cylinder surface. The collision-free regime of the flow around the cylinder was used as a test case. The resultant values of the drag coefficient and heat flux are in good agreement with the values calculated by Eqs. (1) and (2).

2.3. *Drag Coefficient.* Figure 2 shows the drag coefficient calculated as a function of the accommodation coefficient α. It follows from Eq. (1) that the drag coefficient in a free-molecular flow around a cylinder is a linear dependence on α. An analysis of data in Fig. 2 allows us to conclude that the dependence of the drag coefficient on α for other regimes is also close to linear. Some nonlinearity of the curves is observed for $\alpha < 0.25$. The nonlinearity of the curves becomes more pronounced with decreasing Knudsen number.

2.4. *Heat Flux.* Formula (2) predicts a linear dependence of the heat flux on the accommodation coefficient for a free-molecular flow around a cylinder. Let Q be the specific heat flux calculated by summing the kinetic energy of particles that collided with the cylinder surface in a unit time and normalized to the unit area of the cylinder surface. Figure 3 shows the heat flux Q as a function of the ratio of temperatures T_w/T_0 for different values of the Knudsen number and $\alpha = 1.0$, 0.5, and 0.1 ($\mathrm{M}_s = 2.9$). The data obtained show that the heat flux decreases almost linearly with increasing ratio of temperatures T_w/T_0. Naturally, the slope of the curves decreases with decreasing α.

Figure 4 shows the heat flux Q versus α for different values of Kn. In analyzing these data, we can see that linear approximation can only be used for minor changes in α. The nonlinearity becomes more pronounced as the free-stream Mach number increases.

2.5. *Recovery Temperature.* An important characteristic of the gas flow around a cylinder is the recovery temperature T_r (see, e.g., [1, 2]). In a free-molecular flow around a transversely aligned cylinder, the values of T_r are described by the analytical dependence (3). This parameter is used in the theory of hot-wire anemometers [15].

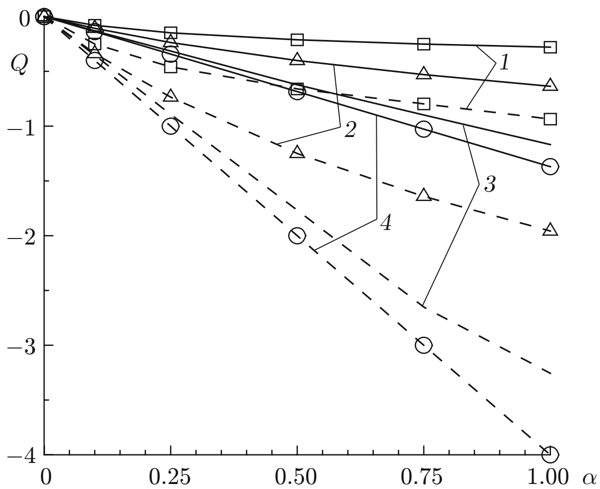

Fig. 4

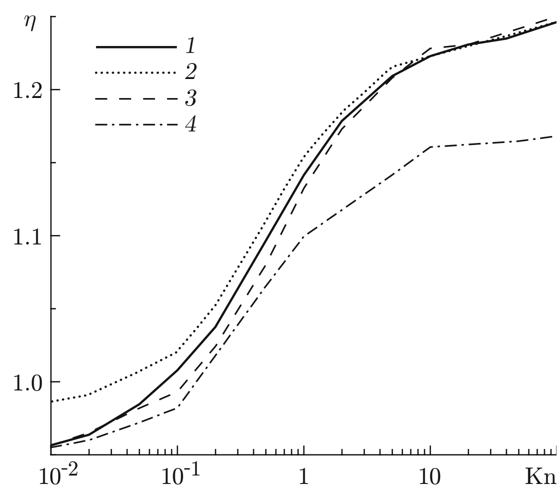

Fig. 5

Fig. 4. Heat flux Q versus the accommodation coefficient α for $T_w/T_0 = 7/3$ and different values of the Knudsen number: the solid and dashed curves refer to $\mathrm{M}_s = 2.9$ and 5.6, respectively; Kn = 0.01 (1), 0.1 (2), 1 (3), and ∞ (4).

Fig. 5. Dimensionless recovery temperature versus Knudsen number: 1) $\mathrm{M}_s = 2.9$ and $\alpha = 1$; 2) $\mathrm{M}_s = 2.9$ and $\alpha = 0.5$; 3) $\mathrm{M}_s = 5.6$ and $\alpha = 1$; 4) data [16] for a diatomic gas flow ($\mathrm{M}_s = 5.9$) around a cylinder.

The expression for the sensitivity of the hot-wire anemometer involves the dimensionless recovery temperature $\eta = T_r/T_0$. In a continuum medium (Kn $\to 0$), we have $\eta \approx 0.96$ [15], and in a free-molecular regime η depends on the Mach number and the number of internal degrees of freedom of gas molecules.

The recovery temperature in the transitional regime was determined by the dependence $Q(T_w/T_0)$ (see Fig. 3). The dependences obtained are close to linear. A point with a zero heat flux was determined on the temperature scale for each dependence. The values at these points were taken as the recovery temperature. Test computations were performed for several thus-obtained recovery temperatures, which showed that the heat flux for these ratios of temperatures T_w/T_0 is close to zero.

Figure 5 shows the dimensionless recovery temperature as a function of the Knudsen number and the data obtained in [16] with the use of the SMILE software system for a diatomic gas (nitrogen) flow with a Mach number $\mathrm{M}_s = 5.9$ around a cylinder. The results computed for Kn = 0.01 are in good agreement with data obtained for a continuum flow, and the results computed for Kn > 40 are consistent with data for a free-molecular flow. For Kn > 10, the Mach number and the accommodation coefficient exert a weak effect on the recovery temperature. The effect of the polyatomic character of the gas is much more pronounced. At low Knudsen numbers, the greatest effect is exerted by the accommodation coefficient. The influence of the Mach number (within the range examined) and of the polyatomic character is insignificant, which agrees with the conclusions drawn in [2, 17].

To analyze the effect of the accommodation coefficient on the recovery temperature in more detail, we plotted the dependence $\eta(\alpha)$ for $\mathrm{M}_s = 2.9$ and 5.6 (Kn = 0.01 and 1.00) (Fig. 6). In a free-molecular flow around a cylinder, the recovery temperature is known to be independent of the accommodation coefficient. If allowance is made for particle collisions, the recovery temperature decreases with increasing α, and this decrease is more significant as the Knudsen number becomes lower.

Figure 7 shows the dependence $\eta^*(\mathrm{Kn})$, where $\eta^* \equiv (\eta - \eta_c)/(\eta^\infty - \eta_c)$, η^∞ is the dimensionless recovery temperature in the case of a free-molecular flow; the parameter η_c is determine by an empirical formula for the case of a continuum flow around a cylinder [17]:

$$\eta_c = 1 - 0.05\,\frac{\mathrm{M}^{3.5}}{1.175 + \mathrm{M}^{3.5}}\ .$$

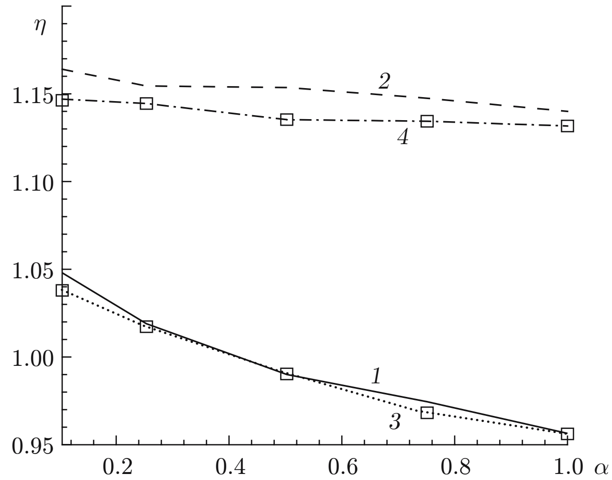

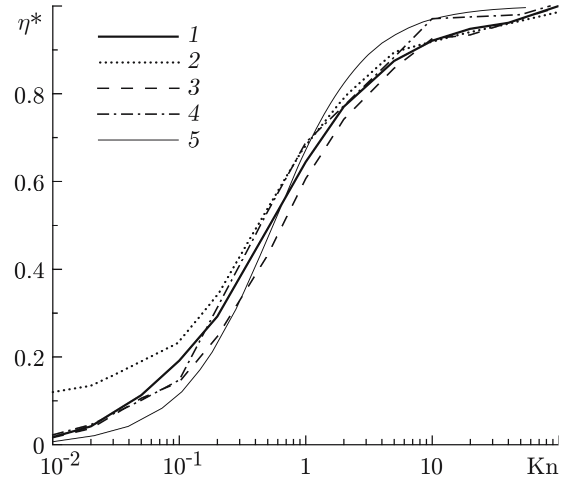

Fig. 6

Fig. 7

Fig. 6. Dependence $\eta(\alpha)$ for $\mathrm{M}_s = 2.9$ (1 and 2) and 5.6 (3 and 4); Kn = 0.01 (1 and 3) and 1 (2 and 4).

Fig. 7. Dependence of η^* on the Knudsen number: 1) $\mathrm{M}_s = 2.9$ and $\alpha = 1$; 2) $\mathrm{M}_s = 2.9$ and $\alpha = 0.5$; 3) $\mathrm{M}_s = 5.6$ and $\alpha = 1$; 4) diatomic gas ($\mathrm{M}_s = 5.9$) [16]; 5) calculation by Eq. (4).

Figure 7 also shows the empirical dependence

$$\eta^* \equiv \frac{\eta - \eta_c}{\eta^\infty - \eta_c} = \frac{\mathrm{Kn}^{1.193}}{0.493 + \mathrm{Kn}^{1.193}}, \tag{4}$$

derived in [17] on the basis of processing a large amount of experimental data obtained for $\gamma = 1.4$ and $\mathrm{M} > 0.4$.

Conclusions. An analysis of the problem based on DSMC simulations allowed us to identify the following important features of the flow field near the cylinder surface.

The most pronounced effect on the distributions of flow macroparameters along the axis of symmetry is exerted by the degree of flow rarefaction. For $\mathrm{Kn} \leqslant 0.1$, a detached shock wave is formed. With a further decrease in Kn, a region with linear changes in flow parameters and a boundary layer depending on the temperature factor and accommodation coefficient are formed behind the detached shock wave.

The length of the region with substantial changes in flow macroparameters ahead of the cylinder (expressed in mean free paths) increases with decreasing Knudsen number and decreases with increasing Mach number and decreasing α.

The drag coefficient C_x decreases with decreasing accommodation coefficient.

At finite values of the Knudsen number and different Mach numbers and accommodation coefficients, the heat flux decreases almost linearly as the ratio of temperatures T_w/T_0 increases. The effect of the temperature factor on the heat flux becomes less pronounced with decreasing Knudsen number.

Linear approximation can be used to describe the dependences $C_x(\alpha)$ and $Q(\alpha)$ only if there are minor changes in α.

At high values of Kn, the Mach number and the accommodation coefficient exert a weak effect on the recovery temperature. The polyatomic character of the gas has a much stronger effect.

At low Knudsen numbers, a significant effect on the recovery temperature is produced by the accommodation coefficient. The influence of the Mach number (in the examined range) and polyatomic character of the gas is insignificant at low Knudsen numbers. With increasing α, the recovery temperature decreases, and this decrease is more pronounced with decreasing Knudsen number.

The author is grateful to A. K. Rebrov and A. A. Morozov for useful discussions of the work performed.

This work was supported by the Russian Foundation for Basic Research (Grant Nos. 06-01-00292 and 06-01-08000), by the Council on Grants of the President of the Russian Federation for Supporting the Leading Scientific Schools (Grant No. NSh-5101.2006.1), and by the Integration Project No. 8.11 of the Presidium of the Russian Academy of Sciences.

REFERENCES

1. M. N. Kogan, *Rarefied Gas Dynamics. Kinetic Theory* [in Russian], Nauka, Moscow (1967).
2. Yu. A. Koshmarov and Yu. A. Ryzhov, *Applied Dynamics of Rarefied Gas* [in Russian], Mashinostroenie, Moscow (1977).
3. V. A. Bashkin, I. V. Yegorov, M. V. Yegorova, and D. V. Ivanov, "Supersonic flow past a circular cylinder with an isothermal surface," *Fluid Dyn.*, **36**, No. 1, 147–153 (2001).
4. A. B. Gorshkov, "Heat transfer in supersonic low-Re flow past a sphere and a cylinder," *ibid.*, pp. 139–146.
5. K. Koura and M. Takahira, "Monte Carlo simulation of hypersonic rarefied nitrogen flow around a circular cylinder," in: *Proc. of the 19th Int. Symp. on Rarefied Gas Dynamics* (Oxford, July 25–29, 1994), Vol. 2, Oxford Univ. Press, Oxford (1995), pp. 1236–1242.
6. G. A. Bird, *Molecular Gas Dynamics and the Direct Simulation of Gas Flows*, Clarendon Press, Oxford (1994).
7. S. L. Gorelov and S. V. Rusakov, "Physicochemical model of hypersonic rarefied gas flow past bodies," *Fluid Dyn.*, **37**, No. 4, 624–636 (2002).
8. M. Yu. Plotnikov and A. K. Rebrov, "Direct statistical simulation of a supersonic flow of a binary mixture of rarefied gases around a transversely positioned cylinder," *J. Appl. Mech. Tech. Phys.*, **46**, No. 5, 658–663 (2005).
9. M. Yu. Plotnikov, "Direct statistical simulation of transverse supersonic rarefied gas flow around a cylinder," *Fluid Dyn.*, **39**, No. 3, 495–502 (2004).
10. A. K. Rebrov, A. A. Morozov, M. Yu. Plotnikov, et al., "Determination of accommodation coefficients of translational and internal energy using a thin wire in free-molecular flow," *Rev. Scient. Instrum.*, **74**, No. 2, 1103–1106 (2003).
11. A. K. Rebrov, A. A. Morozov, M. Yu. Plotnikov, et al., "The accommodation of the translational and rotational energy of a gas in a Knudsen flow past a thin wire," *J. Exp. Theor. Phys.*, **97**, No. 4, 738–744 (2003).
12. A. K. Rebrov, N. I. Timoshenko, and A. V. Shishkin, "Vacuum deposition of thin teflon-like films from a supersonic C_2F_4 jet," *Doklady Physics*, **49**, 739 (2004).
13. A. K. Rebrov, R. S. Sharafudinov, A. V. Shishkin, and N. I. Timoshenko, "Free C_2F_4 jet deposition of thin PTFE-like films," *Plasma Process Polym.*, **2**, No. 6, 464–471 (2005).
14. R. V. Maltsev and A. K. Rebrov, "Gas-dynamic colliders: numerical simulations," *J. Appl. Mech. Tech. Phys.*, **48**, No. 3, 420–427 (2007).
15. V. A. Lebiga, *Hot-Wire Anemometry in Compressible Flows* [in Russian], Izd. Novosib. Gos. Tekh. Univ., Novosibirsk (1997).
16. A. A. Shevyrin, "Analysis of features of a rarefied gas flow in the transitional regime," Master Paper, Novosibirsk (2003).
17. C. F. Dewey, "A correlation of convective heat transfer and recovery temperature data for cylinders in compressible flow," *Int. J. Heat Mass Transfer*, **8**, No. 2, 245–252 (1965).